A Loss-Minimization DTC Scheme for EV Induction Motors

Abdelhakim Haddoun, Mohamed Benbouzid, Demba Diallo, Rachid Abdessemed, Jamel Ghouili, Kamel Srairi

A Loss-Minimization DTC Scheme for EV Induction Motors

A. Haddoun[1], M.E.H. Benbouzid[2], D. Diallo[3], R. Abdessemed[4], J. Ghouili[5] and K. Sraïri[6]
[1]Electrical Engineering Department, University of Oum El Bouaghi, Oum El Bouaghi, Algeria
[2]Laboratoire d'Ingénierie Mécanique et Electrique (LIME), IUT of Brest, University of Western Brittany
Rue de Kergoat – BP 93169, 29231 Brest Cedex 3, France
Phone: +33 2 98 01 90 07 – *Fax*: + 33 2 98 01 66 43 – *E-mail*: m.benbouzid@ieee.org
[3]Laboratoire de Génie Electrique de Paris (LGEP) CNRS UMR 8507 – Supélec, Plateau du Moulon, Paris XI, 91192 Gif-Sur-Yvette, France
[4]Electrical Engineering Department, University of Batna, Batna, Algeria
[5]GRET Research Group, Engineering Faculty, University of Moncton, Moncton, New Brunswick, Canada
[6]Electrical Engineering Department, University of Biskra, Biskra, Algeria

Abstract—**This paper proposes a strategy to minimize the losses of an induction motor propelling and Electric Vehicle (EV). The proposed control strategy, based on a Direct Flux and Torque Control (DTC) scheme, utilizes the stator flux as control variable and the flux level is selected in accordance with torque demand of the EV to achieve the efficiency optimized drive performance. Moreover, among EV's motor electric propulsion features; the energy efficiency is a basic characteristic that is influenced by vehicle dynamics and system architecture. For this reason, the EV dynamics is taken into-account. Simulations tests have been carried out on a 1.1-kW EV induction motor drive to evaluate the consistency and the performance of the proposed control approach.**

Index Terms—**Electric vehicle, induction motor, DTC, loss-minimization.**

I. Introduction

As shown in [1], an EV drive system must feature the following.

– High instant power and high power density.
– High torque at low speeds for starting and climbing, as well as high power at high speed for cruising.
– Very wide speed range including constant-torque and constant-power regions.
– Fast torque response.
– High efficiency over wide speed and torque ranges.
– High efficiency for regenerative braking.
– High reliability and robustness for various vehicle-operating conditions.
– Reasonable cost.

The shortcomings, which caused the EV to lose its early competitive edge, have not yet been totally overcome. Indeed, EVs have a low energy density and long charging time for the present batteries. Therefore, optimal energy management is very important in EVs; in addition optimum design of the motor, selection of a proper drive, and optimal control strategy are the other major factors in EVs.

For EVs propulsion, the cage induction motor seems to be candidate that better fulfils the major above-mentioned features [2]. Induction motor drives control techniques are well treated in the literature. The most popular is the so-called vector control technique that is now used for high impact automotive applications (EV and HEV). In this case, the torque control is extended to transient states and allows better dynamic performances [1], [3]. Among these techniques, DTC appears to be very convenient for EV applications [4-7]. DTC has the advantage of not requiring speed or position encoders and uses voltage and current measurements only. Flux, torque, and speed are estimated. It also has a faster dynamic response due to the absence of the PI current controller. The input of the motor controller is the reference speed, which is directly applied by the pedal of the vehicle.

Furthermore, DTC typical advantages are not sufficient. EVs induction motor drive has also to possess a high efficiency in order to extend the running distance per battery charge. Therefore, DTC should be associated to a loss-minimization strategy so as to maximize the drive efficiency. Indeed, EV motors have a high torque-to-volume ratio and a wide speed operation range [8]. As a consequence, these motors are characterized by their low inductance and high current density, so that they run at high speed and produce a high starting torque. Due to the low inductance coil design, the current ripple caused by PWM switching makes a significant amount of eddy-current losses and hysteresis losses, especially in high-speed operation. If we simply neglect the iron losses, then it detunes the overall vector controller and results in an error in the torque control [9]. Loss-minimization in the induction motor is directly related to the choice of the flux level. The higher the flux level is, the larger the iron losses are. But extreme minimization causes high copper losses. There is an optimal flux level that guarantees loss-minimization. Choosing the level of flux in the induction motor remains an open problem from the perspective of maximizing motor efficiency and many researchers continue to work on this problem. Numerous operation schemes have been proposed by many researchers concerning the optimal choice of excitation current or flux level for a given operating point. In low-frequency operation, core loss (hysteresis and eddy current loss) is rather low compared with copper loss. As the speed goes up, however, the contribution of the eddy current loss increases and finally becomes dominant. Hence, the optimal combination of d-axis and q-axis currents varies, depending on the required torque and speed [10].

Among the above-mentioned motor drive features, the energy efficiency is a basic characteristic that is influenced by vehicle dynamics and system architecture. Therefore, in this paper a detailed dynamic model of an EV is introduced and associated with the proposed loss-minimizing DTC induction motor drive strategy. The objective is here is to test the effectiveness proposed efficiency optimization strategy on the whole vehicle and not on the sole induction motor. Simulations tests have been carried out on a 1.1-kW EV induction motor drive to evaluate the consistency and the performance of the proposed optimization approach.

II. Vehicle Dynamic Analysis

A. Nomenclature

v = vehicle speed;
α = Grade angle;
P_v = Vehicle driving power;
F_w = Road load;
F_{ro} = Rolling resistance force;
F_{sf} = Stokes force or viscous friction force;
F_{ad} = Aerodynamic drag force;
F_{cr} = Climbing and downgrade resistance force;
μ = Tire rolling resistance coefficient ($0.015 < \mu < 0.3$);
m = Vehicle mass;
g = Gravitational acceleration constant;
k_A = Stokes coefficient;
ξ = Air density;
C_w = Aerodynamic drag coefficient ($0.2 < C_w < 0.4$);
A_f = Vehicle frontal area;
v_0 = is the head-wind velocity;
F = Motive force;
k_m = Rotational inertia coefficient ($1.08 < k_m < 1.1$);
a = Vehicle acceleration;
J = Total inertia (rotor and load);
ω_m = Motor mechanical speed;
T_B = Load torque accounting for friction and windage;
T_L = Load torque;
T_{em} = Motor torque;
i = Transmission ratio;
η_t = Transmission efficiency;
R = Wheel radius;
J_V = Shaft inertia moment;
J_W = Wheel inertia moment;
λ = Wheel slip.

B. Dynamics Analysis

Based on principles of vehicle mechanics and aerodynamics, one can assess both the driving power and energy necessary to ensure vehicle operation (Fig. 1) [8], [11-12].

The power P_v required to drive a vehicle at a v speed has to compensate the road load F_w.

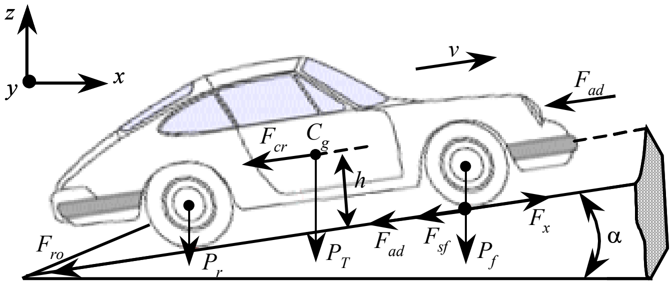

Fig. 1. Elementary forces acting on a vehicle.

$$P_v = vF_w = v(F_{ro} + F_{sf} + F_{ad} + F_{cr}) \quad (1)$$

The rolling resistance force F_{ro} is caused by the tire deformation on the road.

$$F_{ro} = \mu mg\cos\alpha \quad (2)$$

μ is a non linearly dependent of the vehicle speed, type, tire pressure, and road surface characteristic. It increases with vehicle speed and also during vehicle turning maneuvers.

$$F_{sf} = k_A v \quad (3)$$

Aerodynamic drag, F_{ad}, is the viscous resistance of air acting upon the vehicle.

$$F_{ad} = \frac{1}{2}\xi C_w A_f (v + v_0)^2 \quad (4)$$

The climbing resistance (F_{cr} with positive operational sign) and the downgrade force (F_{cr} with negative operational sign) is given by

$$F_{cr} = \pm mg\sin\alpha \quad (5)$$

The motive force F available from the propulsion system is partially consumed in overcoming the road load. The net force (F - F_w), accelerates the vehicle (or decelerates when F_w exceeds F). Therefore, the acceleration is given by

$$a = \frac{dv}{dt} = \frac{F - F_w}{k_m m} \quad (6)$$

The mechanical equation (in the motor referential) used to describe each wheel drive is expressed by

$$J\frac{d\omega_m}{dt} + T_B + T_L = T_{em} \quad (7)$$

The following equation is derived due to the use of a reduction gear.

$$\begin{cases} \omega_{Wheel} = \dfrac{\omega_m}{i} \\ T_{Wheel} = T_m i \eta_t \end{cases} \quad (8)$$

The load torque in the motor referential is given by.

$$T_L = \frac{T_{LWheel}}{i} = \frac{R}{i} F_\omega \quad (9)$$

The vehicle global inertia moment in the motor referential is given by

$$\begin{cases} J = J_W + J_V \\ J_V = \dfrac{1}{2} m \dfrac{R^2}{i^2}(1-\lambda) \end{cases} \quad (10)$$

If the adhesion coefficient of the road surface is high, then λ is usually low and can be neglected.

III. Direct Torque Control

The basic idea of the method is to calculate flux and torque instantaneous values from only the stator variables. Control is carried out by hysteresis comparators and a switching logic table selecting the appropriate voltage inverter switching configurations [6]. Figure 2 gives the global configuration of a DTC scheme and also shows how the EV dynamics will be taken into account.

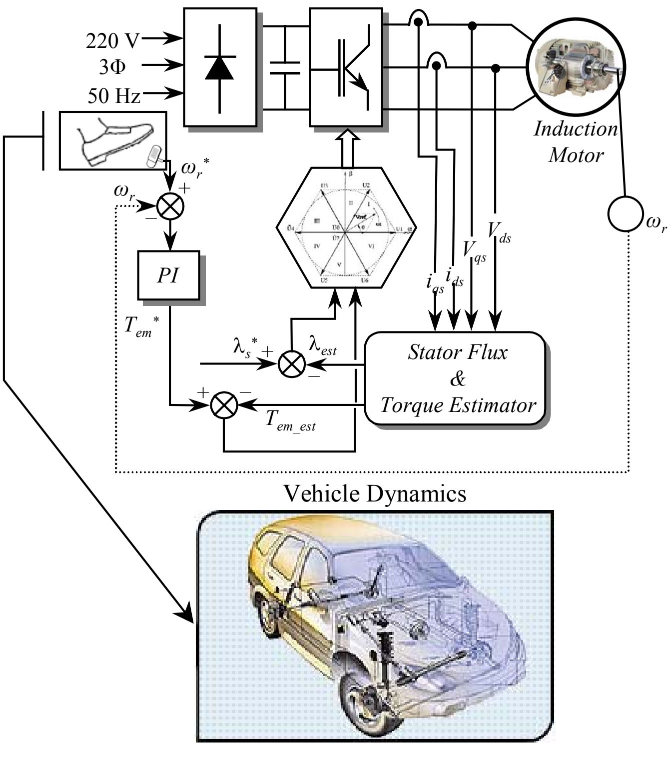

Fig. 2. DTC general configuration.

A. Nomenclature

V_s (V_r) = Stator (rotor) voltage space vector;
λ_s (λ_r) = Stator (rotor) flux space vector;
R_s (R_r) = Stator (rotor) resistance;
L_s (L_r) = Stator (rotor) inductance;
L_m = Mutual inductance;
ω_r = Rotor electric speed;
$\theta_{\lambda s}$ = Stator flux angular position;
p = pole-pair number.

B. Direct Torque Control

The induction motor model in the stator-fixed *d-q* reference frame is described by (while the mechanical equation is (7))

$$\begin{cases} V_s = R_s i_s + \dfrac{d\lambda_s}{dt} \\ V_r = R_r i_r + \dfrac{d\lambda_s}{dt} - j\omega_r \lambda_r \\ \lambda_s = L_s i_s + L_m i_r \\ \lambda_r = L_m i_s + L_r i_r \end{cases} \quad (11)$$

The induction motor stator flux can be estimated as follows.

$$\begin{cases} \lambda_{ds} = \int \left(V_{ds} - R_s i_{ds} \right) dt \\ \lambda_{qs} = \int \left(V_{qs} - R_s i_{qs} \right) dt \\ \left| \lambda_s \right| = \sqrt{\lambda_{ds}^2 + \lambda_{qs}^2} \\ \theta_{\lambda s} = \tan^{-1}\left(\dfrac{\lambda_{qs}}{\lambda_{ds}} \right) \end{cases} \quad (12)$$

Then, the electromagnetic torque is estimated using

$$T_{em} = \frac{3}{2}\frac{p}{2}\left(\lambda_{ds} i_{qs} - \lambda_{qs} i_{ds} \right) \quad (13)$$

IV. Induction Motor Losses Model

A. Nomenclature

R_{fs} = Core loss resistance;
f_s = Stator frequency;
k_h = Hysteresis loss coefficient;
k_f = Eddy current loss coefficient;
S = Per-unit slip;
P_s = stator copper losses;
P_r = Rotor copper losses;
P_{fs} = Core losses;
ω_s = Stator angular velocity;
A = Current ratio ($i_{sq} = A\, i_{sd}$).

B. Losses Model

Stator and rotor copper losses are embedded in the dynamic model of the motor, by means of stator and rotor resistances. Both temperature and skin effect on winding resistances were neglected. The core loss resistance R_{fs} is a function of the frequency and flux level, but it is more sensitive to frequency variation. It is therefore expressed by [9-10]

$$R_{fs} = k_h f_s + k_f f_s^2 \tag{14}$$

This resistance could be neglected at low speed according to R_s value. The corresponding rotor core loss is given by

$$R_{fr} = k_h S f_s + k_f (S f_s)^2 \tag{15}$$

At high speed, the stator flux frequency is almost the same as the speed frequency (the slip frequency is nearly zero and the rotor core losses could be neglected). There are four types of losses in an induction motor propelling an EV: copper core losses in the stator and the rotor. Friction and windage losses are generally neglected. Therefore, the induction motor losses model is given by [13-14]

$$\begin{cases} P_s = R_s\left(i_{sd}^2 + i_{sq}^2\right) \\ P_r = R_r\left(i_{sq} - \dfrac{\omega_s L_m}{R_{fs}} i_{sd}\right)^2 \\ P_{fs} = \left(\omega_s L_m\right)^2 \dfrac{1}{R_{fs}} i_{sd}^2 \end{cases} \tag{16}$$

The losses can be rearranged as

$$\begin{cases} P_{loss,d} = \left(\left(\omega_s L_m\right)^2 \dfrac{1}{R_{fs}} + R_s + \left(\omega_s L_m\right)^2 \dfrac{R_r}{R_{fs}^2}\right) i_{sd}^2 \\ P_{loss,q} = \left(R_r + R_s\right) i_{sq}^2 \\ P_{loss,dq} = -2\omega_s L_m \dfrac{R_r}{R_{fs}} i_{sd} i_{sq} \end{cases} \tag{17}$$

Using the torque expression and the definition of A,

$$T_{em} = pL_m i_{sd} i_{sq}$$

the total losses become

$$P_{loss} = \frac{T_{em}}{pL_m}\left\{\left[\left(\omega_s L_m\right)^2 \frac{1}{R_{fs}} + R_s + \left(\omega_s L_m\right)^2 \frac{R_r}{R_{fs}^2}\right]\frac{1}{A} + \left(R_r + R_s\right) A - 2\omega_s L_m \frac{R_r}{R_{fs}}\right\} \tag{18}$$

Differentiating the losses expression with respect to A and, assuming that the model parameters are independent of A will lead to minimum losses, and particularly to the following

$$P_{loss,d} = P_{loss,q} \tag{19}$$

The induction motor losses are, thus, minimal when the "direct" losses are equal to the "quadrature" losses.

The proposed loss-minimization DTC scheme for an EV is then shown by Fig. 3. In this case, model-based control has the advantage over the simple state control that it can include inverter losses in the calculation.

The principle of the search control is to keep the output power of the motor constant and find the operating point where the input power has a minimum. Measuring the input power and iteratively changing the flux level in small steps until the input power minimum is detected will lead to this minimum. The output power is normally kept constant by keeping the speed constant and assuming a constant load torque [14].

V. Simulation Results

Numerical simulations have been carried out, on an EV propelled by a 1.1-kW induction motor drive which ratings are summarized in the appendix. The objectives of the carried out simulations are to assess the efficiency and dynamic performances of the proposed control strategy.

First, Fig. 4 shows the induction motor flux with and without loss-minimization. In the beginning of the simulation process, the nominal flux is applied to the induction motor drive until it reaches its steady state. When the simulation time reaches 2.3-sec, the loss-minimization strategy is engaged.

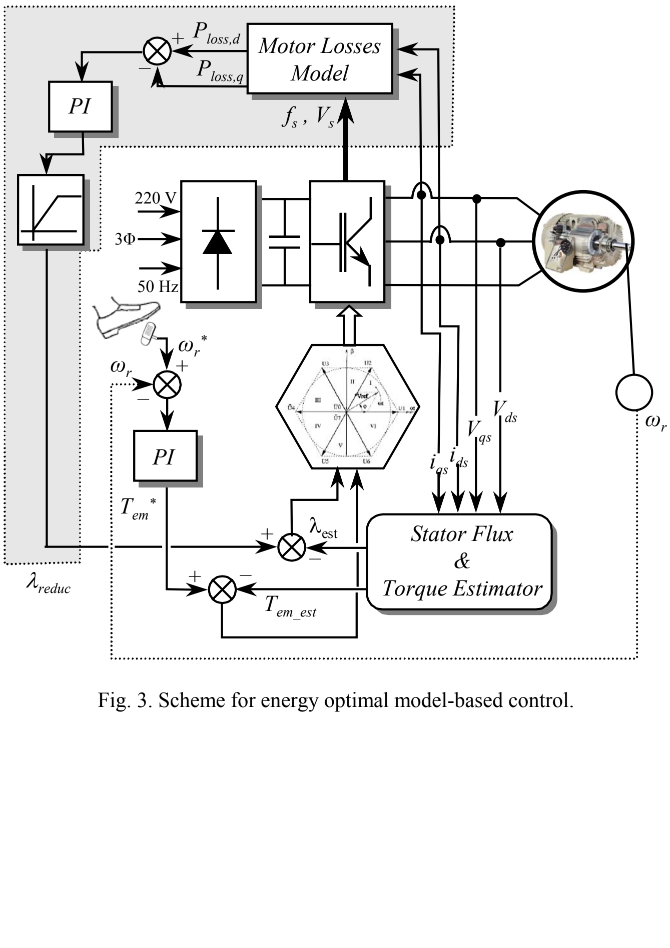

Fig. 3. Scheme for energy optimal model-based control.

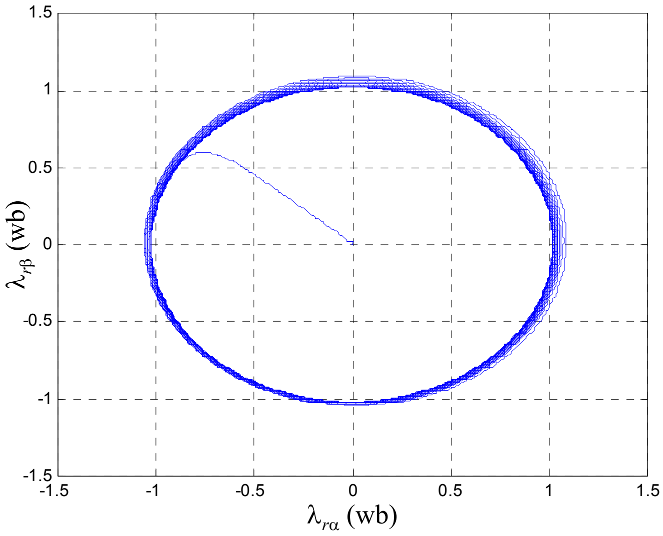

(a) Without optimization.

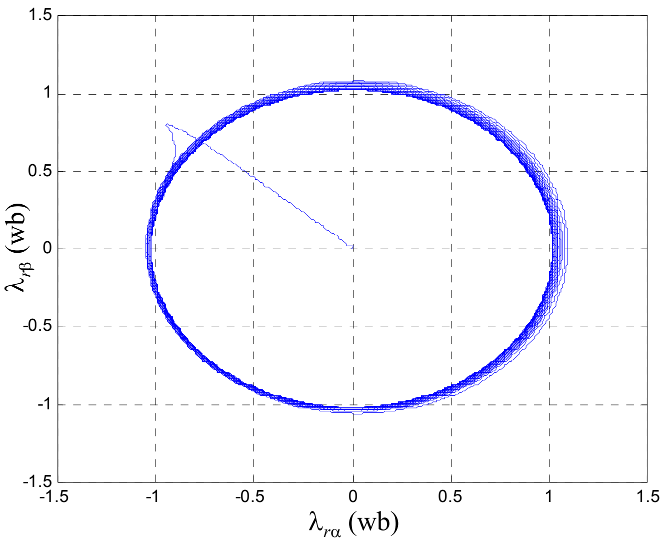

(b) With optimization.

Fig. 4. Flux trajectories.

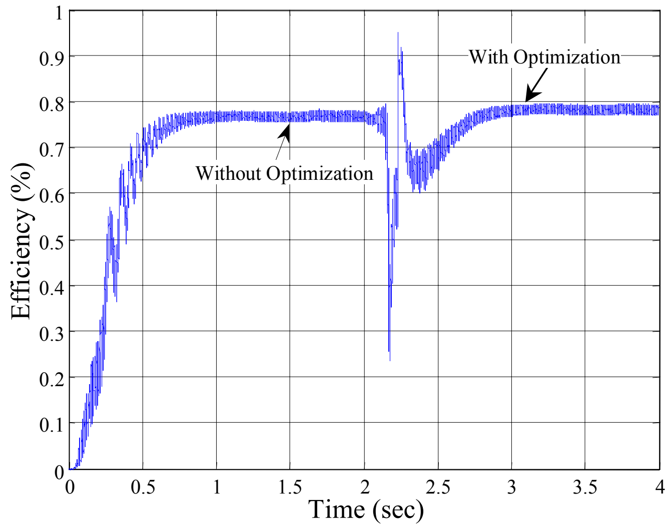

(a) Efficiency.

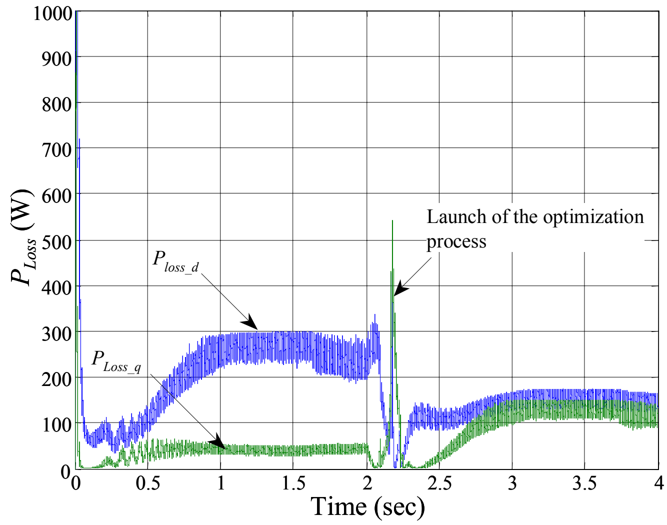

(b) P_{lossd} and P_{lossq} variations.

Fig. 5. Efficiency and power optimization.

Figure 5 illustrates this. Indeed, the obtained results confirm the effectiveness of the optimization process. In fact, Fig. 5a shows that the efficiency increases from 75% to 80% when the flux reaches its optimal value. Moreover, Fig. 5b confirms the principle given by (19).

Figures 6 and 7a, illustrate the EV dynamics, respectively, the electric motor mechanical speed and the developed torque, with changes of the acceleration pedal position and a varied road profile (rising and downward portions). It should be noted that speed and torque variations are as large as are the variations of the accelerator pedal and the road profile. Moreover, Fig. 7 shows that the estimated torque and the developed one are quite indistinguishable, which confirms the good torque control of the induction motor.

VI. Conclusion

This paper presented a detailed dynamic model of an EV that is associated with a loss-minimizing DTC induction motor drive strategy. Compared to previous works, the proposed energy optimization strategy is applied to the whole vehicle, by taking into account its aerodynamics, and not to the sole induction motor. This approach was used to directly minimize the induction motor losses in order to evaluate the optimal magnetizing flux, thus maximizing the efficiency and extending the running distance per battery charge.

Simulations tests that have been carried out on a 1.1-kW EV induction motor drive show that the proposed control approach provides effective loss-minimization control while maintaining a good dynamic response.

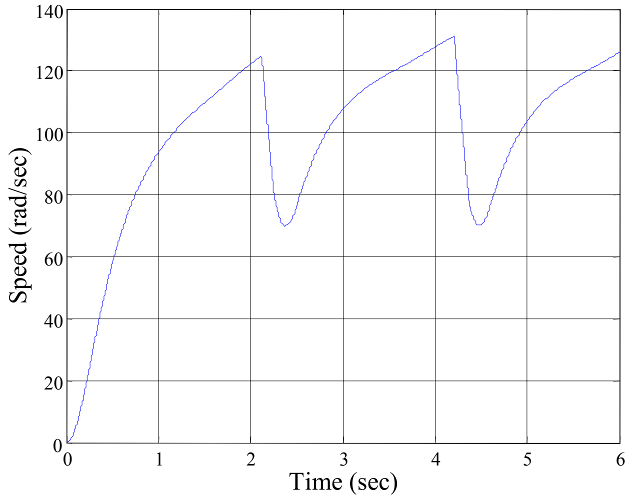

Fig. 6. Speed curve.

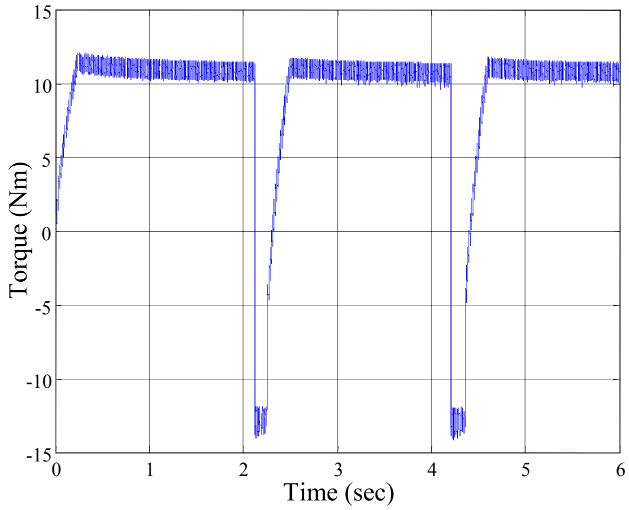

(a) Developed torque.

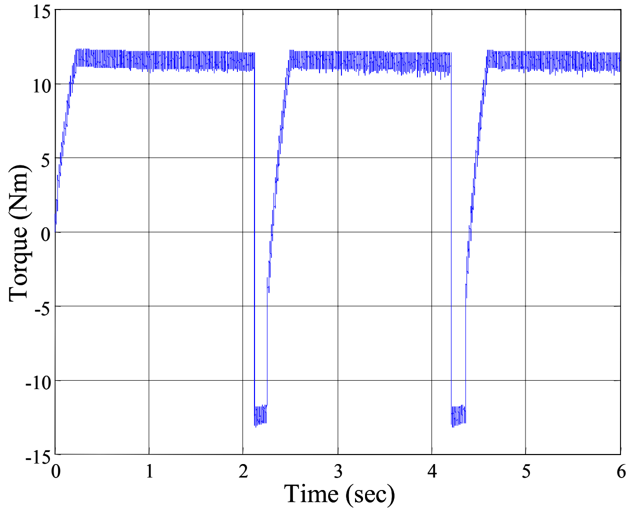

(b) Estimated torque.

Fig. 7. Torque curves.

For applications permanently operating in a steady-state mode, applying this approach would produce significant savings. For tolerant-systems to slight variations in dynamic response, this application would prove to be very efficient.

APPENDIX

RATED DATA OF THE SIMULATED INDUCTION MOTOR

	1.1 kW; 50 Hz; 220/380 V; 5.9/3.4 A; 7 Nm; 1500 rpm $R_s = 8\ \Omega$; $R_r = 3.1\ \Omega$; $L_s = L_r = 0.47$ H, $L_m = 0.443$ H $p = 2$, $J = 0.06$ kg.m²; $\beta = 0.042$ Nm.sec

VEHICLE PARAMETERS

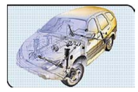	$m = 150$ kg, $A_f = 1$ m^2, $R = 0.23$ m, $\mu = 0.015$, $C_w = 0.25$ $g = 9.81$ m/sec^2, $k_A = 0.22$, $\xi = 0.23$ kg/m^3, $k_m = 1.08$, $i = 5$

REFERENCES

[1] C.C. Chan, "The state of the art of electric and hybrid vehicles," *Proceedings of the IEEE*, vol. 90, n°2, pp. 247-275, February 2002.

[2] M.E.H. Benbouzid et *al.*, "Electric motor drive selection issues for HEV propulsion systems: A comparative study," Paper #10072, *IEEE VPPC'05*, Chicago (Illinois), USA, September 2005.

[3] D.O. Neacsu et *al.*, "Comparative analysis of torque-controlled IM drives with applications in electric and hybrid vehicles vehicle," *IEEE Trans. Power Electronics*, vol. 16, n°2, pp. 240-247, March 2001.

[4] G.S. Buja et *al.*, "Direct torque control of PWM inverter-fed ac motors—A survey," *IEEE Trans. Industrial Electronics*, vol. 51, n°4, pp 744-757, August 2004.

[5] C. Lascu et *al.*, "A sensorless hybrid DTC drive for high-volume low-cost applications," *IEEE Trans. Industrial Electronics*, vol. 51, n°5, pp 1048-1055, October 2004.

[6] J. Faiz et *al.*, "Sensorless direct torque control of induction motors used in electric vehicle," *IEEE Trans. Energy Conversion*, vol. 18, n°1, pp. 1-10, March 2003.

[7] J. Faiz et *al.*, "Different techniques for real time estimation of an Induction motor rotor resistance in sensorless direct torque control for electric vehicle," *IEEE Trans. Energy Conversion*, vol. 16, n°1, pp. 104-109, March 2001.

[8] M. Ehsani et *al.*, "Propulsion system design of electric and hybrid vehicles," *IEEE Trans. Industrial Electronics*, vol. 45, n°1, pp 19-27, February 1997.

[9] J. Jung et *al.*, "A vector control schemes for ev induction motors with a series iron loss model," *IEEE Trans. Industrial Electronics*, vol. 45, n°4, pp. 617-624, August 1998.

[10] S. Lim et *al.*, "Loss-minimising control scheme for induction motor," *IEE Proc.-Electr. Power Appl.*, vol. 151, n°4, pp. 385-397, July 2004.

[11] B. Szadkowski et *al.*, "A study of energy requirements for electric and hybrid vehicles in cities," *in Proceedings of the 2003 International Conference on Clean, Efficient and Safe Urban Transport*, Gdansk. June 4-6, pp 1-8, 2003.

[12] I. Husain et *al.*, "Design, modeling and simulation of an electric vehicle system," *SAE Technical Paper Series*, Paper # 1999-01-1149.

[13] F. Abrahamsen et *al.*, "Efficiency-optimized control of medium-size induction motor drives," *IEEE Trans. Industry Applications*, vol. 37, n°6, pp 1761-1767, November-December 2001.

[14] F. Abrahamsen et *al.*, "On the energy optimized control of standard and high-efficiency induction motors in ct and hvac applications," *IEEE Trans. Industry Applications*, vol. 34, n°4, pp 822-83, July-August 1998.

Abdelhakim HADDOUN was born in Constantine, Algeria, in 1967. He received the *B.Sc.* and the *M.Sc.* degrees in Electrical Engineering, from the University of Batna, Algeria, in 1993 and 1999 respectively. In 2000, he joined the Electrical Engineering Department of the University of Oum El Bouaghi, Algeria, as a Teaching Assistant.

He is currently pursuing the *Ph.D.* degree on electric vehicle control and power management.

Mohamed El Hachemi BENBOUZID (S'92-M'94-SM'98) was born in Batna, Algeria, in 1968. He received the *B.Sc.* degree in Electrical Engineering, in 1990, from the University of Batna, Algeria; the *M.Sc.* and *Ph.D.* degrees both in Electrical and Computer Engineering, from the National Polytechnic Institute of Grenoble, France, in 1991 and 1994 respectively.

After graduation, he joined the University of Picardie "Jules Verne", France, where he was an Associate Professor of Electrical and Computer Engineering at the Professional Institute of Amiens. In November 2000, he received the "*Habilitation à Diriger des Recherches*" degree from the University of Picardie "Jules Verne". In September 2004, he joins the IUT of Brest, University of Western Brittany as a Professor of Electrical Engineering. His main research interests and experience include analysis, design, and control of electric machines, variable speed drives for traction and propulsion applications, and fault diagnosis of electric machines.

Demba DIALLO (M'99) was born in Dakar, Senegal, in 1966. He received the *M.Sc.* and *Ph.D.* degrees both in Electrical and Computer Engineering, from the National Polytechnic Institute of Grenoble, France, in 1990 and 1993 respectively.

From 1994 to 1999, he worked as a Research Engineer in the Laboratoire d'Electrotechnique de Grenoble, France, on electrical drives and active filters (hardware and software). In 1999 he joined the University of Picardie "Jules Verne" as Associate Professor of Electrical engineering. In September 2004, he joins the IUT of Cachan, University of Paris XI as an Associate Professor of Electrical Engineering. He is with the Laboratoire de Génie Electrique de Paris. His current area of research includes advanced control techniques and diagnosis in the field of ac drives.

Rachid ABDESSEMED was born in Batna, Algeria, in 1951. He received the *M.Sc.* and *Ph.D.* degrees in Electrical Engineering, from Kiev Polytechnic Institute, Ukraine, in 1982.

He has been working for more than eighteen years at the University of Batna where he is a Professor in the Electrical Engineering Department. Currently, he is the Director of the Electrical Engineering Laboratory. His current area of research includes design and control of induction machines, reliability, magnetic bearings, and renewable energy.

Jamel GHOUILI was born in Ghardimaou, Tunisia, in 1962. He is currently Professor at the University of Moncton, Canada, where he is responsible of the power electronics and drives Teaching and Research program since 2000. He received the *B.Sc.*, the *M.Sc.* and the *Ph.D.* degrees from University of Québec at Trois-Rivières, Canada, in 1986, 1998 and 2004 respectively. Early in his career, he served as Professor at Ecole Polytechnique de Masuku, Gabon. His main research interests include power converters, ac drives, DSP and FPGA control, sensorless control, EV/HEV drives, fuzzy logic and neural network applications in power electronics and drives.

Kamel SRAIRI was born in Batna, Algeria, in 1967. He received the *B.Sc.* degree in Electrical Engineering, in 1991, from the University of Batna, Algeria; the *M.Sc.* degree in Electrical and Computer Engineering, from the National Polytechnic Institute of Grenoble, France, in 1992; and the *Ph.D.* degree also in Electrical and Computer Engineering, from the University of Nantes, France, in 1996.

After graduation, he joined the University of Biskra, Algeria, where he is an Associate Professor in the Electrical Engineering Department His main research interests include analysis, design, and control of electric machines.